Environmental Science and Pollution Research (2022) 29:58133–58148
https://doi.org/10.1007/s11356-022-19708-8

RESEARCH ARTICLE

$PM_{2.5}$ decadal data in cold vs. mild climate airports: COVID-19 era and a call for sustainable air quality policy

Rodrigo Rangel-Alvarado[1] · Devendra Pal[2] · Parisa Ariya[1,2]

Received: 9 November 2021 / Accepted: 10 March 2022 / Published online: 1 April 2022

Abstract

Airports are identified hotspots for air pollution, notably for fine particles ($PM_{2.5}$) that are pivotal in aerosol-cloud interaction processes of climate change and human health. We herein studied the field observation and statistical analysis of 10-year data of $PM_{2.5}$ and selected emitted co-pollutants (CO, NO_x, and O_3), in the vicinity of three major Canadian airports, with moderate to cold climates. The decadal data analysis indicated that in colder climate airports, pollutants like $PM_{2.5}$ and CO accumulate disproportionally to their emissions in fall and winter, in comparison to airports in milder climates. Decadal daily averages and standard errors of $PM_{2.5}$ concentrations were as follows: Vancouver, 5.31 ± 0.017; Toronto, 6.71 ± 0.199; and Montreal, 7.52 ± 0.023 μg/m^3. The smallest and the coldest airport with the least flights/passengers had the highest $PM_{2.5}$ concentration. QQQ-ICP-MS/MS and HR-S/TEM analysis of aerosols near Montreal Airport indicated a wide range of emerging contaminants (Cd, Mo, Co, As, Ni, Cr, and Pb) ranging from 0.90 to 622 μg/L, which were also observed in the atmosphere. During the lockdown, a pronounced decrease in the concentrations of $PM_{2.5}$ and submicron particles, including nanoparticles, in residential areas close to airports was observed, conforming with the recommended workplace health thresholds ($\sim 2 \times 10^4$ cm^{-3}), while before the lockdown, condensable particles were up to $\sim 1 \times 10^5$ cm^{-3}. Targeted reduction of $PM_{2.5}$ emission is recommended for cold climate regions.

Keywords Airport pollution · Air quality · Particles in snow · Aerosols · Emerging contaminants · COVID-19

Introduction

The World Health Organization (WHO) considers that air pollution kills approximately 7 million people every year worldwide (WHO 2021). Air pollution is composed of gases and suspended particles, or aerosols with diameters of a few nm to several microns. In this paper, we refer to aerosols with a diameter less than 1 micron as submicron, which includes nanoparticles. Aerosols are detrimental to human health and the Earth's climate (Organization 2010; Stocker 2014). Of all air pollutants, smaller aerosols (< 100 nm *aka* nanoparticles) are of major concern for human health. The WHO considers airborne nanoparticles a major cause of premature human mortality in children (Nazarenko et al. 2021; Organization 2014).

The effects of particles on human health depend on their different physical and chemical properties and exposure time. For instance, the deposition of particles in the respiratory system depends on the size of the inhaled particles (Kreyling et al. 2006). Particles of smaller sizes can travel further down the respiratory system (Kreyling et al. 2006). Nanoparticles are considered to have more toxicity on human health as they can be deposited in the alveolar region of the pulmonary system (Yang et al. 2008). Airborne nanoparticles are also the most numerous aerosols (~ > 80%) (Morawska et al. 2008).

Airport-related emissions are the upmost contributors to air pollution in areas near airports (Chauhan and Singh 2020, Mazaheri et al. 2011, Singh and Chauhan 2020), where a vast increase in particulate matter (PM) is observed (Unal et al. 2005). It has been reported that ~ 97% of particles are due to aviation activities, including fine particles or particulate matter with diameters smaller than 2.5 microns

Responsible Editor: Gerhard Lammel

✉ Parisa Ariya
parisa.ariya@mcgill.ca

[1] Department of Chemistry, McGill University, Montréal, QC H3A 2K6, Canada

[2] Department of Atmospheric & Oceanic Sciences, McGill University, Montréal, QC H3A 2K6, Canada

($PM_{2.5}$) (Camero 2019; Mazaheri et al. 2011). Airplane contrails contain soot and other particles emitted from aviation activities, on which water vapor condenses (Kärcher 2018). In airports, a significant source of $PM_{2.5}$, including soot and other carbonaceous aerosols, is fuel burning by jet engines (Stacey 2018). Notwithstanding that airplane fuels are different motor vehicles, mostly using kerosene instead of gasoline fuel, and thus different amounts and types of pollutants (Midcontinent 2021).

Aircraft emissions of $PM_{2.5}$ include soot (Timko et al. 2010), metals, and other organic and inorganic emerging contaminants (Masiol and Harrison 2014, Rahim et al. 2019). Aside from particles, engines exhaust from aircraft produces several toxic gases such as NO_x, CO, SO_2, and other greenhouses gases (Bhattacharjee et al. 2015; Harrison et al. 2015). Airborne particles related to commercial aviation have been shown to be emitted predominantly during aircraft takeoff, landing, or idling activities, thus affecting airport regions (Camero 2019; Mazaheri et al. 2011; Vennam et al. 2017). The aircraft idling practice is not only harmful to human health, but it also is expensive, it can damage the engine, and it is ineffective to warm up the engine (Bern 2019). It has been observed that exposure to particles generated by idling causes inflammation of the bronchial epithelial cells (Jonsdottir et al. 2019).

Jet engine emissions have been associated with health effects in people working at airports (Bendtsen et al. 2021). Exposure to $PM_{2.5}$ from aircraft emissions has shown short-term (Lammers et al. 2020) and long-term (Wing et al. 2020) health effects even on healthy individuals. Annual fossil fuel energy usage by the air traffic industry is estimated to be ~ 3% (Barrett et al. 2010). Black carbon particle emission, which is essential in climate change, is estimated to be approximately $(10.9 \pm 2.1) \times 10^{25}$ annually, with an average emission index of $(6.06 \pm 1.18) \times 10^{14}$ per kg of burned fuel for aviation activities (Zhang et al. 2019), whereas they were estimated for ~ 2.5% of global carbon dioxide (CO_2) emissions. It is notable that the impact of various other pollutant atmospheric distributions such as volatile sulfate and nitrate aerosols perturbed by aviation emissions is uncertain (Brasseur et al. 2016).

A major concern regarding air pollution from airports is the rapid increase of commercial flights every year due to the increased accessibility prior to the COVID-19 pandemic (Bhattacharjee et al. 2015, Chauhan and Singh 2020, Chauhan and Singh 2021). The aviation industry contributes 4% to global warming and 2.4% to CO_2 global emissions (Klöwer et al. 2021). Since 2004, there has been a global increase in the number of flights of about 69.3% (from 23.8 million in 2004 to 40.3 million in 2020 before COVID-19) with an increase of $3.38\% \pm 0.636$ every year (Statista 2021a). Canada has followed the same trend, as shown in Fig. S5, illustrating the increase in the total number of passengers in Canada's three major airports from 2008 to 2019. Toronto's airport is the largest in Canada, followed by Vancouver (Chan 2020) and Montreal (Montreal 2020), with more than 417,228 flights in 2019 (Pearson 2020). In terms of the number of passengers, there has been an increase of 136.9% globally, from 1994 million in 2004 to 4723 million in 2020 (Statista 2021b). In Toronto's airport, the number of passengers in 2014 was ~ 40 million and is expected to increase to ~ 80 million by 2035 (Pearson 2016). Nevertheless, there has been little to no regulation on air pollution emission by aircraft (Harrison et al. 2015). In 2020, however, due to the COVID-19 pandemic, global air traffic has seen a drastic decrease (Statista 2021c), resulting in decreased aircraft-related emissions (Berman and Ebisu 2020). According to a previous study, if the trends prior to COVID-19 resume, it is expected that the global temperature will increase by 0.1 °C by 2015 by the effects of the aviation industry alone (Klöwer et al. 2021).

This research had two goals: (I) evaluate whether 10-year statistical observations of $PM_{2.5}$ in the three largest Canadian airports in cold and mild climates are distinct, and how meteorological factors such as the cold temperature and snowfall in airport areas affect the composition of pollutants in snow, nearby airports; (II) determine whether a pronounced decrease in the concentrations of particles in residential areas close to airports was observed and whether the values are above or below the recommended health thresholds, during the COVID-19 lockdown.

Experimental section

Particle size measurement

We used a condensation particle counter (CPC) model 3007 (TSI Inc.) for field measurements. The CPC does not provide the particle size aggregated information, yet it is a condensation particle counter, providing the number density of particles from 0.01 up to 1.0 µm (TSI 2021).

Sampling location for CPC

The CPC instrument was operated periodically on operation days only from 0.01 to 1.0 µm. Note that equipment can be operated using batteries for two continuous hours. However, the battery can be switched, and the wick can be replenished every 2 h in a public park (Westwood Arena, 750 Avenue Thorncrest, Dorval, QC H9P 2R5) with a community sports center near the airport of Montreal shown in Fig. S1 in the supplementary information, a map of this location has been given.

Snow sample collection

Snow samples were collected near the airport of Montreal in a residential area at 750 Avenue Thorncrest, Dorval, QC H9P 2R5. A travel blank of Milli-Q water was taken for every sampling event. Samples were collected in pre-cleaned gas-tight glass amber jars using sterile equipment and clean suits. Snow samples were collected within 24 h of snowfall from the upper 3 cm of the snowpack. After collection, samples were transported in a cooler packed with snow (for isolation) to the laboratories at McGill University and stored immediately in a freezer at -35 ± 2 °C. Samples were thawed at room temperature just before analysis in clean conditions.

High-resolution scanning transmission electron microscopy with energy-dispersive X-ray spectroscopy (HR-STEM-EDS) and scanning electron microscopy (SEM)

We used HR-STEM-EDS to study the morphology, size, and elemental analysis of particles in snow collected near the airport of Montreal. For analysis, 5 mL of melted snow were deposited on a glow discharged carbon film–coated copper electron microscopy grid. The melted snow was left on the grid for 1 min and then blotted from the grid with the edge of a Kimwipe. Imaging was performed using a FEI Quanta 450 Environmental Scanning Electron Microscope (FE-ESEM) and a FEI Tecnai G2F20 200 kV Cryo-STEM (FEI Electron Optics) equipped with a tungsten filament, at 120 kV. A Gatan Ultrascan 4000 4 k × 4 k CCD Camera System Model 895 was used to acquire the images and an EDAX Octane T Ultra W/ApolloXLT2 SDD and TEAM EDS Analysis System for EDS spectral acquisition.

Chemical analysis of aerosols

Aerosol samples were collected on 19 June 2018 using a Micro Orifice Uniform Deposit Impactor (MOUDI). The instrument was operated for 12 h runs from 6:00 am with a flow rate of 30 L/min. The instrument uses 8 impaction stages to collect size-fractionated aerosol. The concentration of metals in aerosol samples collected near the airport was obtained by ICP/MS/MS. We used a triple quadrupole 8900 Agilent and a SPS 4 auto-sampler, a quartz spray chamber, and a glass concentric nebulizer with a Nickel (Ni) interface cone and the Agilent ICP-(QQQ)-MS/MS MassHunter software for data acquisition. The analysis of metals was done in the He mode with "Low matrix" plasma condition, and auto-tuned lens voltage before each run. The standards used for the analysis were as follows: Agilent particles 8500–6940, High-Purity Standards ICP-(QQQ)-MS/MS-B with concentrations of 10 µg/cm^3. Calibration was done with 2.0% HNO_3 (grade Omnitrace Ultra, EMD) in the range of 0.0–50 mg/m^3. The metal data provided in Table 3 is indeed an average of the absolute concentrations obtained by subtracting a blank filter (without sample) from the sample filter. Triplicate analyses were performed for all samples. We used triplicates at each site. We also used the travelling blanks (Milli-Q water). Furthermore, three filter blanks (for aerosol analysis) have been used for each site and were analyzed three times by ICP-MS.

NAPS site description and instrumentations

Long-term continuous measurement data for NO_x ($NO + NO_2$), CO, O_3, and $PM_{2.5}$ were obtained from the Canadian National Air Pollution Surveillance Program (NAPS) stations from 2008 to 2020. The data for Montreal Airport was obtained from the NAPS station Dorval (Id:50,128, Montreal Airport, coordinates: 45.468322, – 73.741198), while downtown data was collected from station Drummond downtown Montreal (Id:50,105, coordinates: 45.497859, – 73.573035). The data for Vancouver airport was retrieved from Templeton street (Id:100,134, coordinates: 49.186265, – 123.152422), while downtown Vancouver data was obtained from 11th avenue street downtown Vancouver (Id:100,141, coordinates: 49.260267, – 123.077776). The data for Toronto airport was obtained from Jhon street (Id:60,405, coordinates: 43.636390, – 79.392500), and downtown Toronto data was collected from resources road (Id: 60,430, coordinates: 43.709444, – 79.543500). Monthly data was obtained from the City of Montreal Air Quality website. We used the concentrations of $PM_{2.5}$, CO, NO, NO_2, and O_3 measured at the airport of Montreal and its downtown area.

Ozone measurements were performed using a UV-photometric Analyzer (model 49i). Nitrogen oxides' [$NO_x = (NO + NO_2)$] chemiluminescence was evaluated by a NO-NO_2-NO_x Analyzer (Model 42i). Carbon monoxide (CO) was monitored by a trace level enhanced gas filter correlation analyzer (Model 48i-TLE). $PM_{2.5}$ was analyzed using synchronized hybrid ambient real-time analyzers (SHARP 5030) along with the PM2.5 particulates using a Met One SuperSASS-Plus Sequential Speciation Sampler. All equipment was obtained from Thermo Fisher Scientific (Forge Parkway Franklin).

Statistical analysis

In this study, the arithmetic means, standard deviation, standard error, median, 75th, and 25th percentile were calculated for data interpretation. The Spearman correlation coefficients were obtained to see if there was any correlation between variables (downtown vs airport) at each city. We also calculated the Pearson correlation coefficient to verify

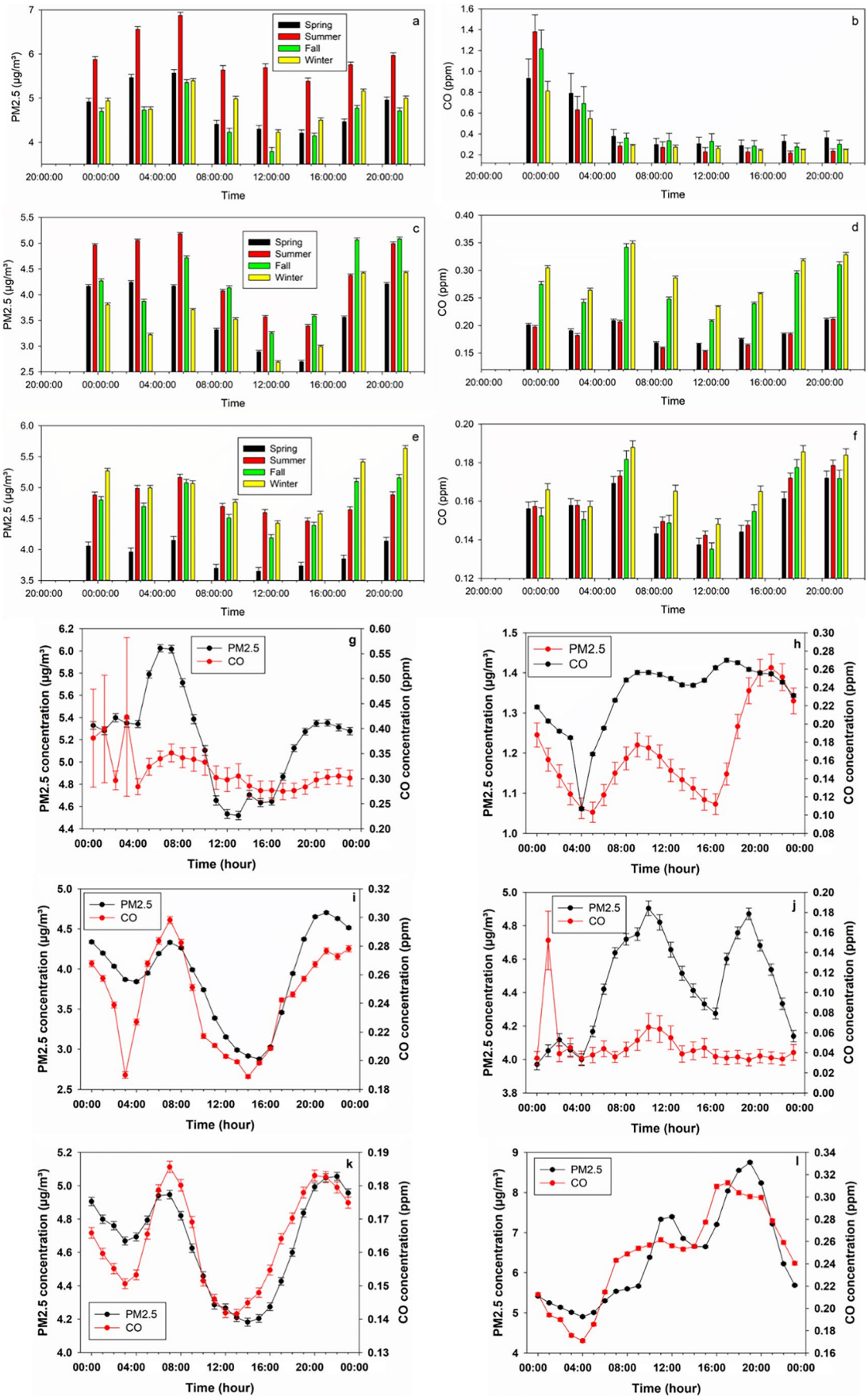
a
PM2.5 (μg/m³)
Spring
Summer
Fall
Winter
Time
b
CO (ppm)
Time
c
PM2.5 (μg/m³)
Spring
Summer
Fall
Winter
Time
d
CO (ppm)
Time
e
PM2.5 (μg/m³)
Spring
Summer
Fall
Winter
Time
f
CO (ppm)
Time
g
PM2.5
CO
PM2.5 concentration (μg/m³)
CO concentration (ppm)
Time (hour)
h
PM2.5
CO
PM2.5 concentration (μg/m³)
CO concentration (ppm)
Time (hour)
i
PM2.5
CO
PM2.5 concentration (μg/m³)
CO concentration (ppm)
Time (hour)
j
PM2.5
CO
PM2.5 concentration (μg/m³)
CO concentration (ppm)
Time (hour)
k
PM2.5
CO
PM2.5 concentration (μg/m³)
CO concentration (ppm)
Time (hour)
l
PM2.5
CO
PM2.5 concentration (μg/m³)
CO concentration (ppm)
Time (hour)

◂**Fig. 1** Seasonal daily mean concentration of **a** $PM_{2.5}$ and **b** CO in Toronto's airport, **c** $PM_{2.5}$ and **d** CO in Vancouver's airport, and **e** $PM_{2.5}$ and **f** CO in Montreal's airport in spring, summer, fall, and winter; and hourly concentration of CO and $PM_{2.5}$ at **g** Toronto's airport and **h** downtown, **i** Vancouver's airport and **j** downtown, and **k** Montreal's airport and **l** downtown. Each data point represents the geometric mean at each hour of the day from January 2008 to December 2019. The error bars represent the standard error calculated as the standard deviation divided by the square root of the total number of samples for each data

the statistical difference of particle size distribution during the lockdown and the year prior. In Montreal, lockdown due to the COVID19 outbreak started on March 13th, and it lasted for about 4 months. On June 22nd, Montreal started partially reopening.

Back-trajectory analysis

To calculate the back trajectories, we used the NOAA HYSPLIT Trajectory Model. The model was run for 25 October 2019 (before COVID lockdown) and 14 April 2020 (after COVID lockdown) at the sampling location near the airport of Montreal, 45.4562° N, 73.7647° W. Each trajectory is for an interval of 24 h.

Materials

All chemicals used for experiments and analyses were purchased from Sigma-Aldrich. The pre-cleaned amber glass jars used for snow sampling were purchased from VWR International. Captiva Premium Syringe Filters with a 0.2 µm pore size, 25 mm wide PES (5190–5275) membrane, were obtained from Agilent Technologies.

Results

Aerosol concentration near airport residential areas

The daily $PM_{2.5}$ particle number density as well as its co-pollutants CO, NO, NO_2, and O_3 at the airports of Toronto, Vancouver, and Montreal for the four different seasons are shown in Fig. 1 and Fig. S2. The time series of these co-pollutants in the three sites are presented in the supplementary material (Fig. S3). An increase of CO, NO, NO_2, and $PM_{2.5}$ were observed during fall and winter, and a decrease of O_3 in all three airports. O_3 is not released directly from anthropogenic activities, unlike the other air pollutants studied in this paper, but it is produced in situ. O_3 is constantly being formed and destroyed when the photolysis of NO_2 produces excited atomic oxygen that reacts with molecular oxygen (O_2) (Crutzen et al. 1999). The remaining NO can react with the newly formed O_3 to regenerate NO_2. Other species, however, can regenerate NO_2 leading to the accumulation of O_3, especially in polluted areas (Edwards et al. 2013). O_3 can also undergo photolysis and react with water vapor to produce OH radicals and O_2. However, the loss of O_3 via these reactions is decreased during winter due to the shorter duration of sunlight and reduced water vapor concentrations (Spivakovsky et al. 2000). In the summertime, the concertation of O_3 also peaks due to photochemical transformation. O_3 generally increases during spring and summer while decreases in fall and winter. Similar results have been reported previously (Rahim et al. 2019), where the change of O_3 is inversely proportional to the change of $PM_{2.5}$ and CO, NO, and NO_2.

Overall, the daily mean concentrations of $PM_{2.5}$ for the 10 years, at the three airports from warmest to coldest, are 5.19 ± 0.017 µg/m^3 in Vancouver, 6.71 ± 0.019 µg/m^3 in Toronto, and 7.34 ± 0.023 µg/m^3 in Montreal. As depicted in Fig. S4, the highest daily average $PM_{2.5}$ concentration was observed in Montreal, even though its airport is the smallest of the three studied airports in Canada, both in terms of flights and number of passengers (Fig. S5). Montreal is also the coldest city, which also receives the most snow each year. Toronto, the largest airport, in terms of travelers and number of flights, and being the second coldest city, has the second largest values of $PM_{2.5}$ daily averages. Vancouver airport which is the second largest airport and is in a coastal mild climate region exhibited the lowest observed average daily $PM_{2.5}$ values. A selected airborne $PM_{2.5}$ emission rate and airborne particle number density in selected airports around the world are given in Tables 1 and 2 for comparison. Airports in Canada are not amongst the airports with the highest airplane traffic and passengers such as Atlanta, Beijing, or Los Angeles; therefore, the $PM_{2.5}$ average concentrations are expected to be lower than the world's largest airports. Yet, as shown in Tables 1 and 2, the average concentration of $PM_{2.5}$ in busy Canadian airports is similar in magnitude to airports like London Heathrow. Despite the difference in the number of passengers (at least Montreal which is more than half), the concentration is barely double.

The average daily concentration trends of $PM_{2.5}$ and CO in the airport of Montreal being higher than Vancouver and Toronto can be explained through the inversion effect of the boundary layers. In cold regions during cold seasons, the bottom layer of the troposphere becomes colder than the upper layers facilitating the entrapment of gas pollutants including particles (Pal et al. 2020). This trend prevails throughout the wintertime (Fig. 1). The inversion effect is stronger in Montreal because Montreal (208 cm average yearly snow) (Canada 2021a) is colder and snowier than Toronto (112 cm average yearly snow) (Canada 2021b), and Vancouver (mild climate city with very limited snow, annual average: 34 cm) (Canada 2021c).

Table 1 Airborne $PM_{2.5}$ concentration and airborne particle number density in selected airports around the world. In absence of data non-applicable acronym is added

Airport	Total passengers in 2019	Airport $PM_{2.5}$ concentration	Airport particle number density	Reference
Montréal-Pierre Elliott Trudeau International Airport	20.3 million	7.52 ± 0.023 μg m^{-3}	2.0×10^6 cm^{-3}	(Rahim et al. 2019) This study
Vancouver International Airport	26.4 million	5.31 ± 0.017 μg m^{-3}	N/A	This study
Toronto Pearson International Airport	50.5 million	6.71 ± 0.199 μg m^{-3}	N/A	This study
Hartsfield-Jackson Atlanta International Airport	110,531,300	25 μg m^{-3} 70 tons $year^{-1}$ (2005)	2.0×10^4 cm^{-3}	(Riley et al. 2016; Unal et al. 2005)
Beijing Capital International Airport	100,011,438	69.35–119.64 μg m^{-3} 149 tons $year^{-1}$ (2018)	N/A	(Zheng et al. 2005) (Yang et al. 2018)
Los Angeles International Airport	88,068,013	33.03 ± 0.15 μg m^{-3}	5.0×10^4 cm^{-3} $(3.9–6.3) \times 10^4$ cm^{-3} $> 10^7$ cm^{-3} (takeoff)	(Hudda and Fruin 2016, Shirmohammadi et al. 2017; Westerdahl et al. 2008; Zhu et al. 2011)
Indira Gandhi International Airport	67,301,016	198.6 ± 55.6 μg m^{-3}	N/A	(Ali et al. 2019)
London Heathrow Airport	80,888,305	11–15 μg m^{-3}	N/A	(Masiol and Harrison 2015)
Shanghai Pudong International Airport	76,153,455	72.2 tons $year^{-1}$ (2020)	N/A	(Xu et al. 2020)
Santa Monica Airport	88,068,013	18 μg m^{-3}	$(1.5–10.6) \times 10^4$ cm^{-3}	(Hu et al. 2009)
Brisbane Airport	24,114,833	1.35×10^4 kg $year^{-1}$	1.98×10^{24} $year^{-1}$ (annual PN)	(Mazaheri et al. 2011)
Amsterdam Airport Schiphol	71,680,000	N/A	$(1.4–4.2) \times 10^4$ cm^{-3} 3.5×10^4 cm^{-3}	(Keuken et al. 2015; Pirhadi et al. 2020)
Copenhagen Airport Kastrup	30,300,00	13–17 μg m^{-3}	$(0.12–3.3) \times 10^4$ cm^{-3}	(Ellermann et al. 2012)
Zurich Airport	31,507,692	N/A	1.04×10^5 cm^{-3}	(Fleuti et al. 2017)
Heathrow Airport	80,800,000	~15 μg m^{-3}	1.9×10^4 cm^{-3} (Masiol et al. 2017)	(Masiol et al. 2017)
Brussels Airport	26,400,000	N/A	$(0.4–3) \times 10^5$ cm^{-3}	(Stacey 2018)
Venice Airport	11,561,594	16 μg m^{-3}	1.4×10^4	(Masiol et al. 2016)
Boston Airport	42,522,411	N/A	1.9×10^4	(Hudda et al. 2018)

The increase of $PM_{2.5}$, CO, NO, and NO_2 during fall and winter is also in part due to the increase of idling of planes (Bern 2019), and the condensation of nanoparticles into larger particles during the cold seasons. As described previously, in cold seasons, cold temperatures alter the air density, and the temperature profile at relatively low altitudes inverts, which result in the accumulation of pollutants near surfaces (Pal et al. 2020). In warmer seasons, the height of the temperature profile at the boundary layer is increased (Argentini et al. 2005), allowing for dilution of air pollutants.

As shown in Fig. 1g–l, an increase of concentration of particles during rush hours (5:00 to 9:00 and 16:00 to 20:00 h) was consistently observed throughout the year regardless of the season with minor fluctuations the rest of the day. The concentration of CO and $PM_{2.5}$ increased during rush hours at the Montreal airport, confirming previous studies (Pal et al. 2020; Rahim et al. 2019). We observed similar trends at rush hours and non-rush hours in all other airports while downtown Vancouver shows otherwise. This is due to the chosen three cosmopolitan cities with diverse meteorology, topography, and climatology. For instance, Montreal is an island, and its meteorology and topography are different from Toronto and Vancouver (Razy et al. 2012). The primary sources in Montreal are vehicle exhaust, local industries, local heating during wintertime, and emissions from restaurants. These sources significantly contributed to $PM_{2.5}$ and CO concentrations (Pal et al. 2020). $PM_{2.5}$ and CO are primarily emitted in the urban atmosphere by traffic emission; thus, both pollutants show strong diurnal dependency in the Montreal region. Similar trends were obtained in the

Table 2 The means, standard deviations, standards errors, median values, 25th percentile values, and 75th percentile values for CO, NO, NO_2, $PM_{2.5}$, and O_3 from January 2008 to December 2019. Pearson's correlation coefficients are obtained between the airport and downtown of each city: Toronto, Vancouver, and Montreal. The Pearson correlation factor and *P*-values between the airport and downtown of each three cities

	Mean	STD	STD error	Median	25%	75%	Pearson's correlation coefficient
$PM_{2.5}$ (μg m^{-3})							
Montreal Airport	7.52	7.31	0.0228	5.86	2.60	10.4	0.569
Montreal Downtown	10.6	8.56	0.0278	8.40	4.75	14.0	$p<0.050$
Vancouver Airport	5.31	5.59	0.0174	4.10	2.30	6.70	0.0409
Vancouver Downtown	9.42	9.01	0.0309	6.60	1.80	15.0	$p<0.050$
Toronto Airport	6.71	59.9	0.199	6.00	3.00	10.0	0.0738
Toronto Downtown	6.33	5.99	0.0193	5.00	2.00	9.00	$p<0.050$
CO (ppm)							
Montreal Airport	0.17	0.12	0.00038	0.17	0.11	0.22	0.294
Montreal Downtown	0.26	0.14	0.00045	0.23	0.17	0.33	$p<0.050$
Vancouver Airport	0.26	0.17	0.00053	0.21	0.16	0.29	0.402
Vancouver Downtown	0.28	0.13	0.00046	0.25	0.20	0.32	$p<0.050$
Toronto Airport	3.29	59.1	0.20	0.22	0.17	0.27	0.00463
Toronto Downtown	0.0235	0.0667	0.00022	0	0	0	$p= 0.164$
NO (ppm)							
Montreal Airport	3.64	11.0	0.03	0.69	0.038	2.49	0.443
Montreal Downtown	8.92	13.0	0.04	4.80	1.82	11.1	$p<0.050$
Vancouver Airport	11.4	24.6	0.08	2.50	0.60	9.40	0.593
Vancouver Downtown	18.8	23.5	0.08	10.4	4.60	23.5	$p<0.050$
Toronto Airport	7.54	63.3	0.21	4.00	1.00	12.0	0.192
Toronto Downtown	3.11	6.50	0.02	1.00	0	3.00	$p<0.050$
NO_2 (ppm)							
Montreal Airport	8.94	9.03	0.03	6.15	2.60	12.48	0.548
Montreal Downtown	15.2	8.76	0.03	13.6	8.68	20.02	$p<0.050$
Vancouver Airport	14.6	9.50	0.0297	12.7	6.70	21.0	0.559
Vancouver Downtown	19.2	7.70	0.0265	18.8	13.4	24.4	$p<0.050$
Toronto Airport	14.1	61.2	0.204	15.0	9.00	24.0	0.135
Toronto Downtown	12.3	9.22	0.0258	11.0	6.00	17.0	$p<0.050$
O_3 (ppm)							
Montreal Airport	21.9	13.7	0.0424	22.7	11.7	31.5	0.703
Montreal Downtown	19.8	11.1	0.0346	19.2	11.6	27.1	$p<0.050$
Vancouver Airport	16.7	12.2	0.0382	16.0	5.10	26.1	0.767
Vancouver Downtown	9.42	9.01	0.0309	6.60	1.80	15.0	$p<0.050$
Toronto Airport	17.3	62.1	0.207	20.0	10.0	30.0	0.194
Toronto Downtown	22.3	14.8	0.0413	23.0	12.0	32.0	$p<0.050$

Toronto area with a weak dependence on each other. It could be understood that major industries are located in Toronto other than the local traffic sources (Jeong et al. 2020; Tsai et al. 2004).

Downtown Vancouver shows distinct trends between $PM_{2.5}$ and CO concentrations, specifically from afternoon to early morning. It could be explained due to the different emission sources and geography of the city of Vancouver. The major sources of air pollution, including $PM_{2.5}$ and CO in Vancouver, include industrial emissions, vehicle emissions and wildfire smoke sources, local traffic, construction, and restaurants. It is also noted that Vancouver is a coastal city, and because of that, sea salt aerosol has a significant contribution to $PM_{2.5}$ along with ship traffic-borne aerosols. In contrast to Montreal and Toronto, these are the two important factors in downtown Vancouver that could cause disagreement with the diurnal variability between $PM_{2.5}$ and CO concentration (Geoff Doerksen et al. 2020).

We noted some similarities (CO and $PM_{2.5}$ increase together at the same hours in the three cities) in the concentration trends of $PM_{2.5}$ and CO in the airport of the three studies cities (Tables 1 and 2), even though the airport of Montreal has lower traffic (in terms of number of passengers) than the other two airports (Fig. S5). In short, the

airport of Montreal has a higher concentration of $PM_{2.5}$ and co-pollutants than Toronto and Vancouver despite being a smaller airport with lower traffic (passengers and flights) due to its colder weather.

Statistically, $PM_{2.5}$ is higher in the downtown areas than near the airport; however, $PM_{2.5}$ is not representative of nanoparticles. Rahim et al. (2019) demonstrated that in Montreal the concentration of nanoparticles inside and near the airport is higher than that of downtown. Keep in mind that most of the mass of $PM_{2.5}$ is related to the mass of the larger particles (Zhao et al. 2020a) and the contribution of nanoparticles is generally small, and the exact contribution and particle size distribution vary depending on different factors like location, local weather conditions, and prevailing particle sources (Rönkkö and Timonen 2019). Rahim et al. (2019) found that the size fraction 180–320 nm was the most abundant. Nanoparticles are more toxic than large particles (Nemmar et al. 2013) in air, so even though the concentration of $PM_{2.5}$ is larger in downtown, air pollution due to particles is more significant near the airport. Additionally, in downtown, most particles are likely coming from road-related emissions, whereas particles near the airport come from aircraft-related emissions, since a recent study showed that road emissions and aircraft-related emissions can be distinguished by their particle size distribution and black carbon concentrations (Austin et al. 2021). Aircraft-related emissions have a relatively smaller fine particle size distribution while road-related emissions have a relatively larger fine particle size distribution (Austin et al. 2021). In terms of black carbon, it has been shown that aviation-related emissions have higher concentrations than road emissions (Li and Ariya 2021).

The Pearson correlation coefficient between downtown and the airport (0.569) is small, suggesting that they are not linearly correlated possibly because the source is not the same. The rest of the co-pollutants have a similar tendency where the downtown area has a higher concentration than the airport. The concentration of CO seems to be the most similar between the downtown areas and the airports. Still, the Pearson correlation coefficients are low (Tables 1 and 2).

Physicochemical analysis of particles in fresh snow

Montreal receives 2.1 m of snow over 5 to 6 months per year. The high-resolution electron microscopy imaging was used to obtain the snow particles morphology and elemental composition determination (using EDS). Using this methodology, we demonstrated that some of the airborne particulate pollutants that have been observed in the air were deposited in snow, namely various metal-containing particles (Ariya et al. 2018).

Snow has been shown to host various types of particles of both organic and inorganic nature, as well as biological particles (Mortazavi et al. 2014, 2019). It has also been shown that the existence of particles can change snow albedo or reflectivity, which directly affects the radiation budget and thus climate change (Conway et al. 1996, Warren and Wiscombe 1980). In this study, we measured fresh falling snow, and surface snow during the snow precipitation, as well as aged snow, with methodology explained elsewhere (Kos and Ariya, 2010, Kos et al. 2014). For instance, high-resolution STEM images and corresponding EDS spectra of fresh falling snow are depicted in Fig. 2. Agglomeration of small particles is shown in Fig. 2a. Both rods and tube-like particles were also observed. Figure 2b illustrates the presence of nanostructures or nanotube-like materials, which have been detected previously in highly polluted areas like oil sand regions (Rangel-Alvarado et al. 2019).

EDS elemental analysis revealed that these particles are mostly composed of carbon, hinting at combustion products (Dikio 2011). Cu peaks are related to TEM grids that are made of copper. Figure 2d and e depict particles collected directly from air. In addition to other types of nano-size particles as shown in Fig. 2, larger micron size particles were also detected (Fig. 2g). The presence of these particles suggests the burning of fossil fuels by engines as carbonaceous nanoparticles are generally produced after such activities (D'Anna 2009). There is evidence showing that nanoparticles are produced by aircraft engines; some are soot particles with graphite-type layers (Moulin et al. 2008) and also iron-bearing nanoparticles originating from impurities in the kerosene fuel used in aircrafts (Gonet and Maher 2019). This is something that does not occur with the combustion of regular gasoline fuel by vehicles.

Particles in Fig. 2 had a more complex composition containing different metals such as Fe, Mn, Mg, and Ti (Fig. 2h and i). Chlorine was also present in some particles (Fig. 2i). Chlorine salts are widely used as de-icing in cold climate cities (Hall et al. 2020). The anthropogenic chlorine is suggested to impact the oxidation potential of the atmosphere in cold urban environments (Baudrimont et al. 2020). It is worth noting that such elements have been previously observed near airports (Pal et al. 2020). Other studies of soils near airports have also revealed the presence of different metals and heavy metals and while the concentrations vary from study to study, all agree that the concentration of these species is elevated (Özkan et al. 2017; Rao et al. 2014; Ray et al. 2012). Since the EDS analysis detection is not sufficient for ultra-trace analysis, we also performed a complementary QQQ-ICP-MS/MS analysis. Table 3 presents various metal analyses in aerosols using ICP-MS/MS. As noted in Fig. 2 and Table 3, ICP-MS/MS analysis confirmed the presence of metals such as Fe, Ti, and Mg which were also detected by EDS.

Triple quad ICP/MS/MS analysis of the aerosols collected near the airport of Montreal revealed a wide range

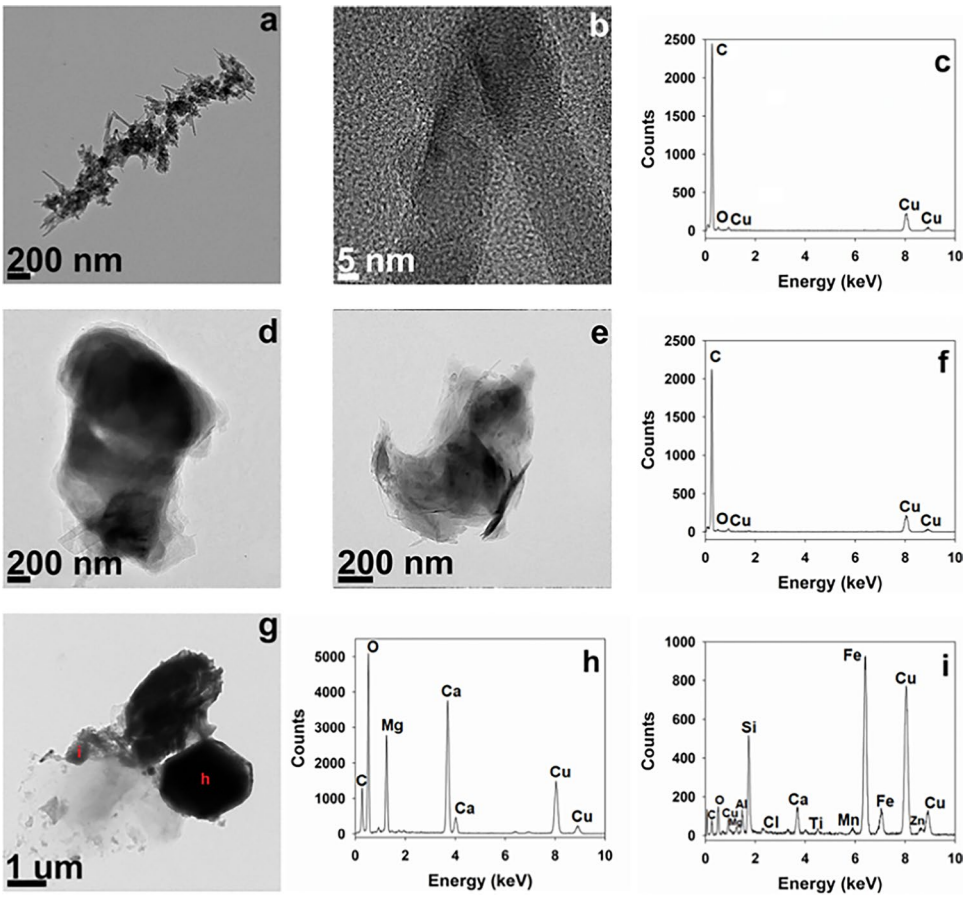

Fig. 2 Electron microscopy images of particles collected near the airport of Montreal, **a** particles in snow containing anthropogenic structures; **b** close-up of a showing a nanotube structure; **c** EDS analysis of **a**; **d** and **e** particles collected directly from air; **f** EDS analysis of **d**; **g** large particle containing a mixture of metals; **h** and **i** EDS analyses of **g**. The Cu signal is from the sample grid

of trace metals, including selected emerging contaminants such as Fe, Ni, Co, and Cr (Stuart and Compton 2015). The reported elevated concentrations of metals in aerosols are in accordance with aerosol measurements, which were observed both in nanoparticles as well as those larger than a micron (Rahim et al. 2019). As shown in Table 3, Al, Fe, and Zn were the most abundant metals observed in aerosols. The concentrations of several transitions and post-transition metals (e.g., Al, Fe, and Zn) were 4.04 up to 28.5 µg/L in the case of Fe. Furthermore, the concentration of metals is not consistently higher at a specific size fraction, for example, particles in the size fraction of 5.6 µm are highest for Ba, Fe, and Al, but not for Zn and other metals. However, fine particles produced by the combustion of fuels are generally enriched by trace metals which are toxic at a high concentration or prolonged exposure (Nelson 2007).

The ICP-MS analysis of particles in the snow has been shown in the airport and the reference site (downtown Montreal, McGill University). We observed that several pollutants are much higher than an already polluted site of downtown Montreal, hinting that the airports are excellent hotspots for the emission of airborne particles found in the air and deposited in snow as shown in the SI (Table S3).

The impact of COVID on airport pollution

In 2020, due to the COVID-19 pandemic, global air traffic has seen a drastic decrease (Statista 2021c), resulting in decreased aircraft-related emissions (Berman and Ebisu 2020). Several studies have reported a decrease in air pollutants such as NO_2, CO, SO_2, and $PM_{2.5}$, and an increase in O_3 in different cities around the world (Briz-Redón et al. 2020, Chauhan and Singh 2020, Kumar et al. 2020, Le et al. 2020, Mishra et al. 2021, Sicard et al. 2020, Siciliano et al. 2020, Zhao et al. 2020b). Figure 3 shows the particle concentration in the airport of Montreal in late 2019 (fall and winter) and early 2020 (winter and spring) before the lockdown was in effect vs the particle concentration during the lockdown period.

During the lockdown period, we observed a drastic decrease in the concentration of particles in the range of 0.01–1.0 µm near the airport of Montreal (Fig. 3a), and of $PM_{2.5}$ (Fig. 3b). This is likely due to the decrease in the number of flights during this period. The concentration of particles before the pandemic in the airport of Montreal has been shown to peak twice a day, between 6:00 and 10:00 am and 4:00 and 8:00 pm (Rahim et al. 2019). During the lockdown period, however, we were unable to

Table 3 Concentration (µg/L) of selected metals in aerosols collected near the airport of Montreal. Each color represents different elemental groups in the periodic table (white: alkali metal; green: transition metals; blue: post-transition metals; and yellow: metalloids). The metal is an absolute concentration obtained by subtracting a blank filter (without sample) from the sampled filter.

Unit	*Size fraction*									
µg /L	**0.18 µm**	**0.32 µm**	**0.56 µm**	**1.0 µm**	**1.8 µm**	**3.2 µm**	**5.6 µm**	**10 µm**	**18 µm**	**LOD**
Alkaline earth metal										
Ba	0.03	0.1	0.21	0.25	0.51	1.01	0.88	0.46	0.14	0.03
Transition metal										
Cr	0.28	0.2	0.05	0.11	0.42	0.26	0.17	0.18	0.36	0.03
Mn	0.17	0.11	0.11	0.11	0.21	0.44	0.5	0.45	0.24	0.03
Fe	28.31	4.04	5.01	6.12	13.98	26.15	28.51	22.83	8.91	0.04
Co	0.02	0.01	0.03	0	0	0.01	0.01	0.02	0	0.04
Ni	0.03	1.12	0.65	0.1	0.07	0.68	0.23	0.25	0.17	0.03
Cu	0	0.1	0.12	0.16	0.36	0.78	0.64	0.38	0.07	0.04
Zn	0.27	16.65	1.04	3.14	0.76	4.22	1.13	1.24	0.52	0.05
Cd	0	0.02	0	0	0	0	0	0	0	0.03
Mo	0.04	0.05	0.01	0.02	0.03	0.03	0.01	0.02	0.02	0.03
Post transition metal										
Al	0.9	4.18	4.04	2.94	5.84	11.22	12.68	10.73	4.04	0.37
Pb	0.03	0.13	0.03	0.02	0.03	0.05	0.05	0.05	0.04	0.03
Metalloids										
As	0.02	0.02	0.01	0	0	0.01	0.01	0.01	0	0.03
Sb	0.01	0.01	0	0	0.02	0.07	0.05	0.01	0.02	0.03

*ND is for concentrations under the detection limit

measure the air-pollutant peaks like previously observed (Rahim et al. 2019), likely due to the sharp decrease in air traffics. Note that hourly, seasonal, and yearly variability in the concentration of submicron particles has been previously observed (Pal et al. 2020; Rahim et al. 2019). As shown in Fig. 3a, there is a significant decrease in condensed particles (0.01–1.0 µm) during the lockdown. We performed statistical analysis (the Pearson correlation coefficient of − 0.259 and *T*-test with a *p*-value < 0.001) indicating the distribution curves prior to and after lockdown are statistically distinct. Note the observational data were taken using a CPC counter on 5 days in October, and 5 days in April at the exact same location close to the Montreal airport. It is particularly interesting, as in cold climates during the winter, fine particles have a large peak in winter, in addition to summer photochemical peaks (Pal et al. 2020). Yet, during the lockdown, a pronounced decrease in the concentrations of $PM_{2.5}$ and submicron, including nanoparticles, in residential areas close to airports was observed ($\sim 1 \times 10^4$ cm^{-3}), while before the lockdown, condensable particles were up to $\sim 1 \times 10^5$ cm^{-3}. Hence, during the lockdown, the highest peak for condensed particles decreased by an order of magnitude, in complete contrast to previous years (Pal et al. 2020).

As illustrated in Fig. 3a, the concentration of particles during the COVID-19 lockdown was below the threshold for health exposure (2 × 104 cm−3) for submicron particles, whereas before COVID-19, it was well above the limits.

It is interesting that the $PM_{2.5}$ trend showed a significant decrease in daily airport peaks of rush hours (both morning and evening, Fig. 3b). Like Fig. 3a, the statistical analysis (the Pearson correlation coefficient of 0.0724 and *T*-test with a *p*-value < 0.001) indicated that the distribution curves prior to and after lockdown are statistically distinct. The difference in Fig. 3b is not as large as Fig. 3a; while the difference in Fig. 3a was at least an order of magnitude, in Fig. 3b, the concentration of $PM_{2.5}$ before and after the lockdown is in the same order of magnitude. Nevertheless, the concentration of $PM_{2.5}$ is lower during the lockdown period similar to other cities (Chauhan and Singh 2020).

The exposure to jet engine emissions is an increasing health concern (Bendtsen et al. 2021; Stettler et al. 2011). Passengers and airport staff are at risk of exposure to these

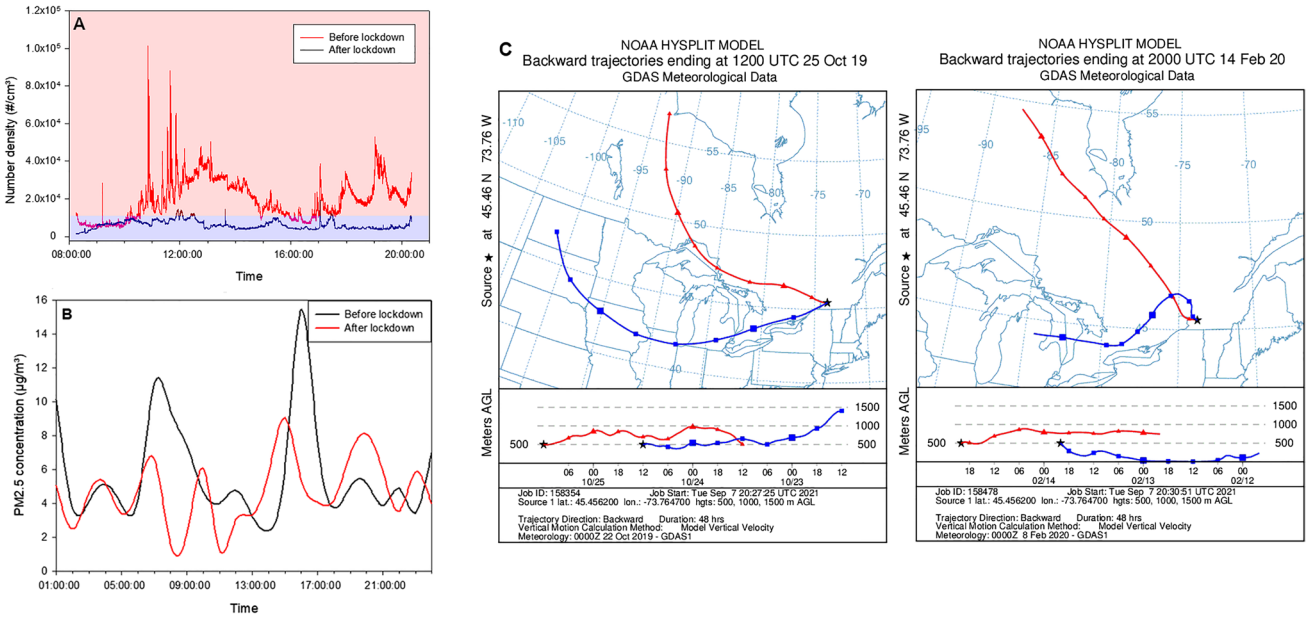

Fig. 3 Daily average **a** particle number density of condensable particles near Montreal Airport as measured by a CPC before lockdown and during lockdown. The $PM_{2.5}$ limit of exposure of 2×10^4 particles/cm^3 is represented by a different color (Dunn et al. 2020; IFA 2012; Van Broekhuizen et al. 2012); **b** $PM_{2.5}$ near Montreal Airport before lockdown and during lockdown; and **c** an example of back-trajectory analysis for the observation of condensable particles as given in Fig. 3a, in a location near the airport of Montreal on the 25 October 2019 and 14 February 2020, during the sampling period. A total of 4 trajectories in a span of 48 h were calculated for both days with an interval of 24 h for each trajectory. The calculations ended at 12:00 am of the selected day

emissions especially particulate matter. In many airports, the concentration of $PM_{2.5}$ can easily reach levels harmful to human health (Bendtsen et al. 2021); for example, Fig. S6 shows the $PM_{2.5}$ concentration in Toronto, Vancouver, and Montreal in 2019 vs 2020. The WHO recommends an annual mean exposure limit to $PM_{2.5}$ of 10 µg/m^3 and a 24-h mean exposure of 25 µg/m^3 (WHO 2018). The exposure limit to airborne particles varies; for example, in Germany, the recommended workplace health threshold is 2×10^4 particles/cm^3 (Dunn et al. 2020; IFA 2012; Van Broekhuizen et al. 2012). Figure 3a illustrates that the particle concentration during the lockdown drops to 2×10^4 particles/cm^3. This concentration has not been reached at least in the past 5 years (Rahim et al. 2019). The drop in concentration due to COVID-19 reveals how much pollution is generated at the airport during normal activities and how much pollution workers and residents of the area are exposed to, especially during cold seasons.

Importance of micrometeorology, topography, and cold climate

We performed trajectory analysis for further understanding of meteorology prior to and during the COVID-19 lockdown. An example of back-trajectory analysis is given in Fig. 3c showing that most of the air masses were coming from the west and northwest. In this example, the observation of condensable submicron particles was done in a location near the airport of Montreal (Fig. S1; a community sports center) on the 25 October 2019 and 14 February 2020, representing the period before and during the COVID-19 lockdown. A total of 4 trajectories in a span of 48 h were calculated for both days with an interval of 24 h for each trajectory. The calculations ended at 12:00 am of the selected day. Notwithstanding that there is clearly variability in wind trajectories, yet, they are typical trajectories where air masses come from the airport. Henry-L'Heureux et al. (2021) demonstrated that at the airport of Montreal the dominant wind direction is from the southwest and that the impacts of the emissions of CO, NO_x, and PM coming from the airport are heavily affected by wind especially the dominant winds.

The island of Montreal has a hill of only 234 m near its center. With such topography, pollution levels are greatly influenced by weather conditions such as the dominant winds (Morera-Gómez et al. 2021). Crucial meteorological factors that distinguish Montreal from other large Canadian urban areas (e.g., Toronto and Vancouver) are the dominance of shallow (~ 1 km) boundary layers during north–northeastern surface wind regimes (Razy et al. 2012), during which selected gases and aerosol concentrations are three times those associated with boundary layers extending to

700 hPa, which are typical of other Canadian urban areas (Razy et al. 2012).

It is possible that the particles found in the samples come from the engine exhaust of planes, as previously suggested (Rahim et al. 2019), as part of the airport of Montreal is located northwest of the sampling location and a residential area with low local traffic is located to the west (Rahim et al. 2019) and plane trajectories from/to the airport include the sampling area. Moreover, strong winds are more frequent in winter (Henry-L'Heureux et al. 2021). Thereby in winter, it results in a faster dispersion of pollutants, resulting in higher pollutant concentrations at the surface in winter than in summer (Henry-L'Heureux et al. 2021). Further research is required to better understand the interactions of particulate pollutants dynamics in cold climate.

Conclusions

The current air quality policy around the world near pollution hotspots does not consider the impact of cold temperature or snow effects. About a third of the planet's land and many cities receive frozen precipitation every year, and thus, it is important to consider the uniqueness of the cold climate airports. Airborne particulate matter, specifically $PM_{2.5}$ as well as nano-sized particles, is mostly emitted during the takeoff and landing of airplanes (Camero 2019; Mazaheri et al. 2011; Zhu et al. 2011), in contrast to some gaseous pollutants that are continuously emitted during the flight. Hence, airport regions are highly affected by particulate matter throughout the year. Notwithstanding that since $PM_{2.5}$ measurements are based on masses, and thus heavier particles that are a less abundant group of aerosol account for most of the mass. It is thus important to measure size aggregated number density of nano-size particles, which are by far the most abundant aerosols.

We showed that the impact of cold temperatures in the entrapment of airborne particles including emerging contaminants has potential for adverse impacts, taking place in the cold seasons such as fall and winter. We provided evidence that during cold temperature seasons some of the particulate pollutions due to airplane activities are indeed transferred to snow. Since it has been shown that snow-air–water/soil photobiochemical interactions occur (Ariya et al. 2018, 2011; Mortazavi et al. 2015; Nazarenko et al. 2017), upon snowmelt, some parts of these particles or their transformed compounds enter the air, affecting adversely the air quality in these neighborhoods.

We hence propose to:

- Implement a regulatory air quality policy for the health threshold of 2×10^4 cm^{-3} for particles in the airport and the residential areas around it to assure the health and safety of airport workers, residents, and passengers.
- Create a targeted quality policy to reduce fine particle emission as recommended for cold/snowy regions, namely during the cold seasons.
- Provide a sustainable airport/aerospace policy to improve human health and living and working conditions around airports in cold climate regions. It is noteworthy that there are new methods to distinguish between aviation and traffic fine particle emissions (Austin et al., 2021).
- Reduce airport particle emission during de-icing procedures in cold climate airports by employing sustainable technological advances, and the reduction of the usage of more sustainable fuels for airplanes.

Supplementary Information The online version contains supplementary material available at https://doi.org/10.1007/s11356-022-19708-8.

Acknowledgements We thank Drs. Melancon and Godefroy of the City of Montreal for providing the access to NAPS data during the COVID-19 and their collaborations.

Author contribution R. R.: formal analysis; investigation; writing—original draft; writing—review and editing; visualization. D. P.: resources, data curation. P. A.: conceptualization; validation; writing—review and editing; visualization; supervision; project administration; funding acquisition.

Funding We received financial support from the Natural Sciences and Engineering Research Council of Canada, from Ville de Montréal, and from Environment and Climate Change Canada.

Data availability All data used for this paper will be made available upon request to the corresponding author Parisa A. Ariya (parisa.ariya@mcgill.ca). The datasets generated and/or analyzed during the current study are available in the cities' repositories:
http://www.airqualityontario.com/history/index.php
http://ville.montreal.qc.ca/portal/page?_pageid=7237,74687650&_dad=portal&_schema=PORTAL
https://catalogue.data.gov.bc.ca/dataset/77eeadf4-0c19-48bf-a47a-fa9eef01f409

Declarations

Ethics approval and consent to participate We declare that we have no human participants or human data.

Consent for publication Not applicable.

Competing interests The authors declare no competing interests.

References

Ali K, Acharja P, Trivedi D, Kulkarni R, Pithani P, Safai P, Chate D, Ghude S, Jenamani R, Rajeevan M (2019) Characterization and

source identification of PM2. 5 and its chemical and carbonaceous constituents during Winter Fog Experiment 2015–16 at Indira Gandhi International Airport. Delhi Sci Total Environ 662:687–696

Argentini S, Viola A, Sempreviva A, Petenko I (2005) Summer boundary-layer height at the plateau site of Dome'C, Antarctica. Bound-Layer Meteorol 115:409–422

Ariya PA, Domine F, Kos G, Amyot M, Côté V, Vali H, Lauzier T, Kuhs W, Techmer K, Heinrichs T (2011) Snow–a photobiochemical exchange platform for volatile and semi-volatile organic compounds with the atmosphere. Environ Chem 8:62–73

Ariya PA, Dastoor A, Nazarenko Y, Amyot M (2018) Do snow and ice alter urban air quality? Atmos Environ 186:266–268

Austin E, Xiang J, Gould TR, Shirai JH, Yun S, Yost MG, Larson TV, Seto E (2021) Distinct ultrafine particle profiles associated with aircraft and roadway traffic. Environ Sci Technol 55:2847–2858

Barrett SR, Britter RE, Waitz IA (2010) Global mortality attributable to aircraft cruise emissions. Environ Sci Technol 44:7736–7742

Baudrimont M, Arini A, Guégan C, Venel Z, Gigault J, Pedrono B, Prunier J, Maurice L, Ter Halle A, Feurtet-Mazel A (2020) Ecotoxicity of polyethylene nanoplastics from the North Atlantic oceanic gyre on freshwater and marine organisms (microalgae and filter-feeding bivalves). Environ Sci Pollut Res 27:3746–3755

Bendtsen KM, Bengtsen E, Saber AT, Vogel U (2021) A review of health effects associated with exposure to jet engine emissions in and around airports. Environ Health 20:1–21

Berman JD, Ebisu K (2020) Changes in US air pollution during the COVID-19 pandemic. Sci Total Environ 739:139864

Bhattacharjee PS, Singh RP, Nédélec P (2015) Vertical profiles of carbon monoxide and ozone from MOZAIC aircraft over Delhi, India during 2003–2005. Meteorol Atmos Phys 127:229–240

Brasseur GP, Gupta M, Anderson BE, Balasubramanian S, Barrett S, Duda D, Fleming G, Forster PM, Fuglestvedt J, Gettelman A (2016) Impact of aviation on climate: FAA's Aviation Climate Change Research Initiative (ACCRI) phase II. Bull Am Meteor Soc 97:561–583

Briz-Redón Á, Belenguer-Sapiña C, Serrano-Aroca Á (2020) Changes in air pollution during COVID-19 lockdown in Spain: a multi-city study. J Environ Sci 101:16–26

Camero (2019) Aviation's dirty secret: airplane contrails are a surprisingly potent cause of global warming. In: SienceMag. https://www.science.org/content/article/aviation-s-dirty-secret-airplane-contrails-are-surprisingly-potent-cause-global-warming#:~:text=The%20aviation%20industry%20has%20long,set%20to%20triple%20by%202050. Accessed 20 Sept 2020

Canda Weather Stats (2021a) Snowfall - Annual data for Montréal. In: Canda Weather Stats. https://montreal.weatherstats.ca/charts/snow-yearly.html. Accessed 10 May 2021

Canda Weather Stats (2021b) Snowfall - Annual data for Toronto. In: Canda Weather Stats. https://toronto.weatherstats.ca/charts/snow-yearly.html. Accessed 10 May 2021

Canda Weather Stats (2021c) Snowfall - Annual data for Vancouver. In: Canda Weather Stats. https://vancouver.weatherstats.ca/charts/snow-yearly.html. Accessed 10 May 2021

Chan (2020) Record 26.4 million passengers at Vancouver International Airport in 2019. In: Urbanized. https://dailyhive.com/vancouver/vancouver-international-airport-2019-passenger-statistics. Accessed 24 February 2021

Chauhan A, Singh RP (2020) Decline in PM2. 5 concentrations over major cities around the world associated with COVID-19. Environ Res 187:109634

Chauhan A, Singh RP (2021) Effect of lockdown on HCHO and trace gases over India during March 2020. Aerosol Air Qual Res 21:200445

Conway H, Gades A, Raymond C (1996) Albedo of dirty snow during conditions of melt. Water Resour Res 32:1713–1718

Crutzen PJ, Lawrence MG, Pöschl U (1999) On the background photochemistry of tropospheric ozone. Tellus b: Chem Phys Meteorol 51:123–146

D'Anna A (2009) Combustion-formed nanoparticles. Proc Combust Inst 32:593–613

Dikio ED (2011) Morphological characterization of soot from the atmospheric combustion of kerosene. E-J Chem 8:1068–1073

Dunn KL, Hammond D, Menchaca K, Roth G, Dunn KH (2020) Reducing ultrafine particulate emission from multiple 3D printers in an office environment using a prototype engineering control. J Nanopart Res 22:1–11

Edwards P, Young C, Aikin K, DeGouw J, Dubé W, Geiger F, Gilman J, Helmig D, Holloway J, Kercher J (2013) Ozone photochemistry in an oil and natural gas extraction region during winter: simulations of a snow-free season in the Uintah Basin, Utah. Atmos Chem Phys 13:8955–8971

Ellermann et al (2012) Assessment of the air quality at the apron of Copenhagen Airport Kastrup in relation to the working environment. In: DCE - Nationalt Center for Miljø og Energi. https://dce.au.dk/udgivelser/tr/nr-1-49/abstracts/no-15-assessment-of-the-air-quality-at-the-apron-of-copenhagen-airport-kastrup-in-relation-to-the-working-environment/. Accessed 24 Feb 2021

Fleuti et al (2017) Ultrafine Particle Measurements
At Zurich Airport. In: zurich-airport.com. https://www.adra-bale-mulhouse.fr/wp-content/uploads/2021/07/PUF_Mesures_Zurich_201703.pdf. Accessed 20 Oct 2020

Doerksen et al. (2020) Metro Vancouver Near-Road Air Quality Monitoring Study. In: Metro Vancouver. http://www.metrovancouver.org/services/air-quality/AirQualityPublications/MV_Near-Road_Air_Quality_Monitoring_Study-Technical_Report.pdf. Accessed 24 Feb 2021

Gonet T, Maher BA (2019) Airborne, vehicle-derived Fe-bearing nanoparticles in the urban environment: a review. Environ Sci Technol 53:9970–9991

Hall R, Nepotchatykh O, Nepotchatykh E, Ariya PA (2020) Anthropogenic photolabile chlorine in the cold-climate city of Montreal. Atmosphere 11:812

Harrison RM, Masiol M, Vardoulakis S (2015) Civil aviation, air pollution and human health. Environ Res Lett 10:041001

Henry-L'Heureux T, Seers P, Ghedhaïfi W, Garnier F (2021) Overview of emissions at Montreal's Pierre Elliott Trudeau international airport and impact of local weather on related pollutant concentrations. Water Air Soil Pollut 232:1–17

Hu S, Fruin S, Kozawa K, Mara S, Winer AM, Paulson SE (2009) Aircraft emission impacts in a neighborhood adjacent to a general aviation airport in Southern California. Environ Sci Technol 43:8039–8045

Hudda N, Fruin S (2016) International airport impacts to air quality: size and related properties of large increases in ultrafine particle number concentrations. Environ Sci Technol 50:3362–3370

Hudda N, Simon M, Zamore W, Durant J (2018) Aviation-related impacts on ultrafine particle number concentrations outside and inside residences near an airport. Environ Sci Technol 52:1765–1772

IFA (2012) Criteria for assessment of the effectiveness of protective measures. In: institut für arbeitsschutz der deutschen gesetzlichen unfallversicherung. https://www.dguv.de/ifa/fachinfos/nanopartikel-am-arbeitsplatz/beurteilung-von-schutzmassnahmen/index-2.jsp. Accessed 20 Sept 2020

Jeong C-H, Traub A, Huang A, Hilker N, Wang JM, Herod D, Dabek-Zlotorzynska E, Celo V, Evans GJ (2020) Long-term analysis of PM2. 5 from,2004 to 2017 in Toronto: Composition, sources, and oxidative potential. Environ Pollut 263:114652

Jonsdottir HR, Delaval M, Leni Z, Keller A, Brem BT, Siegerist F, Schönenberger D, Durdina L, Elser M, Burtscher H (2019) Non-volatile particle emissions from aircraft turbine engines at ground-idle induce oxidative stress in bronchial cells. Commun Biol 2:90

Kärcher B (2018) Formation and radiative forcing of contrail cirrus. Nat Commun 9:1824

Keuken M, Moerman M, Zandveld P, Henzing J, Hoek G (2015) Total and size-resolved particle number and black carbon concentrations in urban areas near Schiphol airport (the Netherlands). Atmos Environ 104:132–142

Klöwer et al (2021) Quantifying aviation's contribution to global warming. Environ Res Lett 16, 10

Kos G, Kanthasami V, Adechina N, Ariya PA (2014) Volatile organic compounds in Arctic snow: concentrations and implications for atmospheric processes. Environ Sci Process Impacts 16:2592–2603

Kos G, Ariya P (2010) Volatile organic compounds in snow in the Quebec-Windsor Corridor. Journal of Geophysical Research: Atmospheres 115

Kreyling WG, Semmler-Behnke M, Möller W (2006) Health implications of nanoparticles. J Nanopart Res 8:543–562

Kumar P, Hama S, Omidvarborna H, Sharma A, Sahani J, Abhijith K, Debele SE, Zavala-Reyes JC, Barwise Y, Tiwari A (2020) Temporary reduction in fine particulate matter due to 'anthropogenic emissions switch-off' during COVID-19 lockdown in Indian cities. Sustainable cities and society 62:102382

Lammers A, Janssen N, Boere A, Berger M, Longo C, Vijverberg S, Neerincx A, Maitland-van der Zee A, Cassee F (2020) Effects of short-term exposures to ultrafine particles near an airport in healthy subjects. Environment international 141:105779

Le T, Wang Y, Liu L, Yang J, Yung YL, Li G, Seinfeld JH (2020) Unexpected air pollution with marked emission reductions during the COVID-19 outbreak in China. Science 369:702–706

Li H, Ariya PA (2021) Black Carbon Particles Physicochemical real-time dataset in a Cold City: Trends of Fall-Winter BC Accumulation and COVID-19. Journal of Geophysical Research: Atmospheres 126, 22

Masiol M, Harrison RM (2014) Aircraft engine exhaust emissions and other airport-related contributions to ambient air pollution: a review. Atmos Environ 95:409–455

Masiol M, Harrison RM (2015) Quantification of air quality impacts of London Heathrow Airport (UK) from 2005 to 2012. Atmos Environ 116:308–319

Masiol M, Vu TV, Beddows DC, Harrison RM (2016) Source apportionment of wide range particle size spectra and black carbon collected at the airport of Venice (Italy). Atmos Environ 139:56–74

Masiol M, Harrison RM, Vu TV, Beddows D (2017) Sources of submicrometre particles near a major international airport. Atmos Chem Phys 17:12379–12403

Mazaheri M, Johnson G, Morawska L (2011) An inventory of particle and gaseous emissions from large aircraft thrust engine operations at an airport. Atmos Environ 45:3500–3507

Midcontinent (2021) Aviation fuel vs. gasoline. In: Midcontinent. https://www.mcico.com/jet-fuel-vs-gasoline. Accessed 24 Feb 2021

Mishra R, Chauhan A, Singh RP, Mishra N, Mishra R (2021) Improvement of atmospheric pollution in the capital cities of US during COVID-19. Modeling Earth Systems and Environment 1, 18

Aeroports de Montreal (2020) Annual Report 2020. In: ADM. https://www.admtl.com/en/adm/medias/publications. Accessed 24 Feb 2021

Morawska L, Ristovski Z, Jayaratne E, Keogh DU, Ling X (2008) Ambient nano and ultrafine particles from motor vehicle emissions: characteristics, ambient processing and implications on human exposure. Atmos Environ 42:8113–8138

Morera-Gómez Y, Cong Z, Widory D (2021) Carbonaceous fractions contents and carbon stable isotope compositions of aerosols collected in the atmosphere of Montreal (Canada): seasonality, sources, and implications. Front Environ Sci 9:86

Mortazavi R, Attiya S, Ariya P (2014) A next generation sequencing of Arctic bacteria in snow and frost flowers: identification, abundance and freezing nucleation. Atmos Chem and Phys Discuss 14:32093–32131

Mortazavi R, Attiya S, Ariya P (2015) Arctic microbial and next-generation sequencing approach for bacteria in snow and frost flowers: selected identification, abundance and freezing nucleation. Atmos Chem Phys 15:6183–6204

Mortazavi R, Attiya S, Ariya PA (2019) Diversity of metals and metal-interactive bacterial populations in different types of Arctic snow and frost flowers: implications on snow freeze-melt processes in a changing climate. Sci Total Environ 690:277–289

Moulin F, Devel M, Picaud S (2008) Optical properties of soot nanoparticles. J Quant Spectrosc Radiat Transfer 109:1791–1801

Nazarenko Y, Fournier S, Kurien U, Rangel-Alvarado RB, Nepotchatykh O, Seers P, Ariya PA (2017) Role of snow in the fate of gaseous and particulate exhaust pollutants from gasoline-powered vehicles. Environ Pollut 223:665–675

Nazarenko Y, Pal D, Ariya PA (2021) Air quality standards for the concentration of particulate matter 2.5, global descriptive analysis. Bull World Health Organ 99:125-137D

Nelson PF (2007) Trace metal emissions in fine particles from coal combustion. Energy Fuels 21:477–484

Nemmar A, Holme JA, Rosas I, Schwarze PE, Alfaro-Moreno E (2013) Recent advances in particulate matter and nanoparticle toxicology: a review of the in vivo and in vitro studies. BioMed Res Int 2013

Organization WH (2014) 7 million premature deaths annually linked to air pollution. World Health Organization, Geneva, Switzerland

World Health Organization (2010) Parma declaration on Environment and Health, Fifth Ministerial Conference on Environment and Health. Protecting children's health in a changing environment

Özkan A, Özkan V, Sungur Ş, Birses H (2017) Heavy metal pollution around international hatay airport. Natural and Engineering Sciences 2:18–24

Pal D, Dastoor A, Ariya PA (2020) Aerosols in an urban cold climate: physical and chemical characteristics of nanoparticles. Urban Clim 34:100713

Toronto Pearson (2016) Growing Canada with a Mega Hub Airport. In: Toronto Pearson International Airport. https://mc-141e1d14-533e-4918-9b8b-7335-cd.azurewebsites.net/-/media/project/pearson/content/corporate/our-future/pdfs/growing-canada-with-a-mega-hub-report.pdf?modified=00010101000000. Accessed 10 May 2021

Toronto Pearson (2020) Airport and market facts. In: Toronto Pearson International Airport. https://www.torontopearson.com/en/corporate/partnering-with-us/air-services/airport-and-market-facts. Accessed 10 May 2021

Pirhadi M, Mousavi A, Sowlat MH, Janssen NA, Cassee FR, Sioutas C (2020) Relative contributions of a major international airport activities and other urban sources to the particle number concentrations (PNCs) at a nearby monitoring site. Environ Pollut 260:114027

Rahim MF, Pal D, Ariya PA (2019) Physicochemical studies of aerosols at Montreal Trudeau Airport: the importance of airborne nanoparticles containing metal contaminants. Environ Pollut 246:734–744

Rangel-Alvarado RB, Willis CE, Kirk JL, St Louis VL, Amyot M, Bélanger D, Ariya PA (2019) Athabasca oil sands region snow

contains efficient micron and nano-sized ice nucleating particles. Environ Pollut 252:289–295
Rao P, Zhu A, Yao W, Zhang W, Men Y, Ding G (2014) Sources and risk assessment of metal contamination in soils at the international airport of Shanghai, China. Toxicol Environ Chem 96:1153–1161
Ray S, Khillare P, Kim K-H (2012) The effect of aircraft traffic emissions on the soil surface contamination analysis around the international airport in Delhi, India. Asian J Atmos Environ 6:118–126
Razy A, Milrad SM, Atallah EH, Gyakum JR (2012) Synoptic-scale environments conducive to orographic impacts on cold-season surface wind regimes at Montreal, Quebec. J Appl Meteorol Climatol 51:598–616
Riley EA, Gould T, Hartin K, Fruin SA, Simpson CD, Yost MG, Larson T (2016) Ultrafine particle size as a tracer for aircraft turbine emissions. Atmos Environ 139:20–29
Rönkkö T, Timonen H (2019) Overview of sources and characteristics of nanoparticles in urban traffic-influenced areas. J Alzheimers Dis 72:15–28
Shirmohammadi F, Sowlat MH, Hasheminassab S, Saffari A, Ban-Weiss G, Sioutas C (2017) Emission rates of particle number, mass and black carbon by the Los Angeles International Airport (LAX) and its impact on air quality in Los Angeles. Atmos Environ 151:82–93
Sicard P, De Marco A, Agathokleous E, Feng Z, Xu X, Paoletti E, Rodriguez JJD, Calatayud V (2020) Amplified ozone pollution in cities during the COVID-19 lockdown. Sci Total Environ 735:139542
Siciliano B, Dantas G, da Silva CM, Arbilla G (2020) Increased ozone levels during the COVID-19 lockdown: analysis for the city of Rio de Janeiro Brazil. Sci Total Environ 737:139765
Singh RP, Chauhan A (2020) Impact of lockdown on air quality in India during COVID-19 pandemic. Air Qual Atmos Health 13:921–928
Spivakovsky C, Logan J, Montzka S, Balkanski Y, Foreman-Fowler M, Jones D, Horowitz L, Fusco A, Brenninkmeijer C, Prather M (2000) Three-dimensional climatological distribution of tropospheric OH: update and evaluation. J Geophys Res Atmos 105:8931–8980
Stacey B (2019) Measurement of ultrafine particles at airports: a review. Atmospheric Environment 198
Statista (2021a) Number of flights performed by the global airline industry from 2004 to 2021. In: statista.com. https://www.statista.com/statistics/564769/airline-industry-number-of-flights/. Accessed 30 July 2021
Statista (2021b) Number of scheduled passengers boarded by the global airline industry from 2004 to 2021. In: statista.com. https://www.statista.com/statistics/564769/airline-industry-number-of-flights/. Accessed 30 July 2021
Statista (2021c) Year-on-year change of weekly flight frequency of global airlines from January 6 to January 4, 2021, by country. In: statista.com. https://www.statista.com/statistics/1104036/novel-coronavirus-weekly-flights-change-airlines-region/. Accessed 30 July 2021
Stettler M, Eastham S, Barrett S (2011) Air quality and public health impacts of UK airports Part i: emissions. Atmos Environ 45:5415–5424
Stocker T (2014) ed. Climate change 2013: the physical science basis: Working Group I contribution to the Fifth assessment report of the Intergovernmental Panel on Climate Change. Cambridge university press, Cambridge, United Kingdom
Stuart EJ and Compton RG (2015) Nanoparticles-emerging contaminants, Environmental Analysis by Electrochemical Sensors and Biosensors. Springer, New York, NY, pp 855–878
Timko MT, Onasch TB, Northway MJ, Jayne JT, Canagaratna MR, Herndon SC, Wood EC, Miake-Lye RC, Knighton WB (2010) Gas turbine engine emissions—Part II: chemical properties of particulate matter. Journal of Engineering for Gas Turbines and Power 132
Tsai J, Owega S, Evans G, Jervis R, Fila M, Tan P, Malpica O (2004) Chemical composition and source apportionment of Toronto summertime urban fine aerosol (PM 2.5). J Radioanal Nucl Chem 259:193–197
TSI (2021) Condensation particle counter 3007. In: TSI. https://tsi.com/products/particle-counters-and-detectors/condensation-particlecounters/condensation-particle-counter-3007/. Accessed 20 Sept 2020
Unal A, Hu Y, Chang ME, Odman MT, Russell AG (2005) Airport related emissions and impacts on air quality: application to the Atlanta International Airport. Atmos Environ 39:5787–5798
University of Bern (2019) Particulate matter from aircraft engines affects airways. In: ScienceDaily. https://www.sciencedaily.com/releases/2019/05/190516114627.htm#:~:text=Summary%3A,particles%20emitted%20during%20ground%20idling. Accessed 20 Sept 2020
Van Broekhuizen P, Van Veelen W, Streekstra W-H, Schulte P, Reijnders L (2012) Exposure limits for nanoparticles: report of an international workshop on nano reference values. Ann Occup Hyg 56:515–524
Vennam L, Vizuete W, Talgo K, Omary M, Binkowski F, Xing J, Mathur R, Arunachalam S (2017) Modeled full-flight aircraft emissions impacts on air quality and their sensitivity to grid resolution. J Geophys Res Atmos 122:13472–13494
Warren SG, Wiscombe WJ (1980) A model for the spectral albedo of snow. II: snow containing atmospheric aerosols. J Atmos Sci 37:2734–2745
Westerdahl D, Fruin SA, Fine PL, Sioutas C (2008) The Los Angeles International Airport as a source of ultrafine particles and other pollutants to nearby communities. Atmos Environ 42:3143–3155
World Health Organization (2018) Ambient (outdoor) air pollution. In: who.int. https://www.who.int/news-room/fact-sheets/detail/ambient-(outdoor)-air-quality-and-health. Accessed 30 July 2021
World Health Organization (2021) Air pollution. In: who.int. https://www.who.int/health-topics/air-pollution#tab=tab_1. Accessed 30 July 2021
Wing SE, Larson TV, Hudda N, Boonyarattaphan S, Fruin S, Ritz B (2020) Preterm birth among infants exposed to in utero ultrafine particles from aircraft emissions. Environ Health Perspect 128:047002
Xu H, Fu Q, Yu Y, Liu Q, Pan J, Cheng J, Wang Z, Liu L (2020) Quantifying aircraft emissions of Shanghai Pudong International Airport with aircraft ground operational data. Environ Pollut 261:114115
Yang W, Peters JI, Williams RO III (2008) Inhaled nanoparticles—a current review. Int J Pharm 356:239–247
Yang X, Cheng S, Lang J, Xu R, Lv Z (2018) Characterization of aircraft emissions and air quality impacts of an international airport. J Environ Sci 72:198–207
Zhang X, Chen X, Wang J (2019) A number-based inventory of size-resolved black carbon particle emissions by global civil aviation. Nat Commun 10:1–11
Zhao Y, Zhang K, Xu X, Shen H, Zhu X, Zhang Y, Hu Y, Shen G (2020b) Substantial changes in nitrogen dioxide and ozone after excluding meteorological impacts during the COVID-19 outbreak in mainland China. Environ Sci Technol Lett 7:402–408
Zhao J, Birmili W, Wehner B, Daniels A, Weinhold K, Wang L, Merkel M, Kecorius S, Tuch T, Franck U (2020a) Particle mass concentrations and number size distributions in 40 homes in Germany:

indoor-to-outdoor relationships, diurnal and seasonal variation. Aerosol and Air Quality Research

Zheng M, Salmon LG, Schauer JJ, Zeng L, Kiang C, Zhang Y, Cass GR (2005) Seasonal trends in PM2. 5 source contributions in Beijing. China Atmos Environ 39:3967–3976

Zhu Y, Fanning E, Yu RC, Zhang Q, Froines JR (2011) Aircraft emissions and local air quality impacts from takeoff activities at a large International Airport. Atmos Environ 45:6526–6533